Analysis of Laser Triangulation Technique Applied to Experimental Deformation of Farm Machinery Elements[1]

Kelen Cristiane Cardoso[2], Daniel Albiero[3], Angelo Roberto Biasi[4], Jonathan Gazzola[5]*, Inacio Maria Dal Fabbro[6]

ABSTRACT - Deformation intensity analysis for mechanical parts are very important data for machine design. For farm machines, these parameters present difficulties for determination due to its particularities. The Machinery industry searches for advanced technologies to determine the mechanical behavior of parts. This article shows the analysis of the reliability in the application of the laser triangulation technique (LTT) to determine the deformation of the mechanical elements of farm machines. A flat cutting disc with standardized dimension was selected as the object of study, as it is commonly used in farm machines, exhibiting a simple geometry made of steel, making the analysis procedure easier both for experimental execution and for data validation. Displacements of 1.0 mm to 10 mm were applied on the specimen. The theoretical behavior of specimen displacement was defined by finite element modelling with same condition of loading and dimension to compare the generated data by the experimental tests. Results indicated a displacement with maximum variation of 2.56% between experimental data and theoretical results and were considered satisfactory. LTT was able to determine deformation curve behavior of machine elements. It was concluded that Laser Triangulation Technique (LTT) was satisfactory to determine the deformation of a specimen.

Key words: Design optimization. Farm machinery elements. Laser triangulation technique. Plan cutting disk. Photomechanics.

INTRODUCTION

In agricultural science, mainly in farm machinery design and development, the occurrence of force intensities and motion analysis, as well as stress and strain association analysis applied to product optimization are very common (CARDOSO; GAZZOLA; DAL FABBRO, 2014; ZULLKIFLI *et al*., 2020). The machinery industry is in search of advanced technologies for its development and optimization that show good results and effective cost (NATRAYAN *et al*., 2019). The use of new analysis effort methods has brought new possibilities for the optimization and development of farm machines (KESNER *et al*., 2021).

Several studies have used practical results for farm machinery projects, comparing theoretical data obtained by computer simulations with real data in order to analyze their influence on the dimensioning of parts and on the understanding of their failures. Niemczewski *et al*. (2014) conducted a study comparing deformation of seeder chassis using finite element method and real deformation data. The study showed that the deformation values obtained were effective and could be applied in the project. However, in the deformation data obtained there was variation between 4% and 35% depending on the digital model adopted for analysis (NIEMCZEWSKI *et al*., 2014). Gürsoy, Chen and Li (2017) analyzed the soil displacement by cutting tools (sweep) and compared it with the real results; they reported the difference between theoretical and practical results. Kesner *et al*. (2021) analyzed soil stresses in agricultural implements using finite and discrete element methods, comparing them with practical results obtained by strain gages. Results obtained were in common agreement between practical and theoretical data with divergences in voltage levels considered acceptable. Xie *et al*. (2018) performed a mixed system of practical experimental data and computer simulation to optimize designs for cutting tools used to harvest sugarcane. Mazzeti *et al*. (2004) mapped complete field displacement of sugarcane circular rotors by applying photomechanical techniques. Results showed different mechanical behavior in function of rotational speed.

Digital image correlation is an area of research related to full-field measurements of strain using non-contact optical techniques to provide efficient and accurate strength data for inelastic materials (HUAN *et al*., 2020; PAN, 2018). The Laser Triangulation Technique (LTT) is a low-cost, high-efficiency, non-contact optical technique that has been widely used in industry to obtain dimensional measurements with regular and irregular shapes, using a surface scan for three-dimensional surveying of objects (DONG *et al*., 2018; SIEKANSKI *et al*., 2019). The technique uses the projection of laser light on the surface, and its movement of images between two points of laser light intensity can measure their displacements (KIENLE *et al*., 2020; MORENO-OLIVA *et al*., 2019). LTT can be applied to obtain displacement and position measurements (XIANG *et al*., 2017). Moreno-Oliva *et al*. (2021) applied LTT to analyze the vibrational displacement of turbine blades to analyze their oscillatory motion. Results found that this technique showed high accuracy. Shen, Li and Luo (2013) analyzed the use of the Laser Speckle Triangulation technique to determine deformations. Results showed that there is a strong accuracy in the data obtained with errors that did not exceed 2% (SHEN; LI; LUO, 2013).

The objective of this article is to analyze the reliability of using the LTT to determine the deformation of agricultural mechanical elements. The element selected for study is a flat cutting disc, commonly used in farm machinery, with simple geometry and metallic material, which makes the analysis procedure easier for experimental execution and validation.

MATERIAL AND METHODS

The experimental tests were carried out at the School of Agricultural Engineering at UNICAMP, Campinas, SP, Brazil. The specimen was represented by a flat disc plane as its geometry is particularly simple for the development of the study, and it represents a part commonly used in farm machinery. The specimen was constituted of steel type SAE J 1269-42 CrMo4 (modulus of elasticity from 109 GPa to 210 GPa, Poison's ratio from 0.27 to 0.30, yielding stress of 1400 MPa), dimensioned of 3.30 mm thick and 360.00 mm in diameter with a central hole of 40.00 and painted with white opaque color. The experimental test was divided into two fronts, namely: 1 – mechanical loading test; 2 – image acquisition and processing.

Mechanical Loading Test

The experimental mechanical loading was realized by EMIC DL30000 testing press with 300 kN capacity baring a displacement transducer. The plate was statically supported in its edge by a disk supporting frame, and the loading was applied at the center of the disk. The optical experiment was carried concomitantly with experimental loading, which employed the use of a 632 nm of 10 mW red diode laser to perform the laser triangulation method and a Samsung Cam CN OS 6,4 Mega pixel Full HD remote controlled to record the images. Fig. 1 shows the experimental setup as described before. A laser line was projected onto the disk surface with an angle of 45° above the digital camera to capture both the non-deformed and the deformed object image.

Figure 1 - Experimental Setup for Laser Triangulation Test
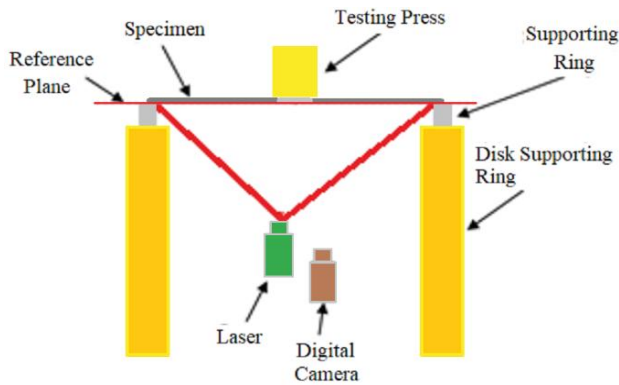
Source: Prepared by author (2021)

This study foresees a possibility of deformation on metallic support during the loading test, which may interfere with the deformation data of the metallic disc. For data correction purposes, a digital dial gauge Mitutoyo Model 543-682 was attached to the structure of the universal testing machine using magnetic support with its measuring tip placed on the lower base of the metallic support to measure its axial displacement during the load test.

Image Acquisition and Processing

The procedure for capturing images for digital processing was performed as described below: first, an image of the non-deformed specimen with the laser line projected under its surface was obtained through the digital camera, becoming an image of the plane of reference, and named as $I_0(x, y)$. Afterwards, the specimen loading test was initiated. A load was applied to the center of the disk and its modulus was determined as a function of the axial displacement of the load cell. Such displacement was measured by the transducers of the universal machine and programmed so that the loading rate was interrupted for each 1 mm of displacement, fixing its position for a period to capture the image of the deformed body by the digital camera, activated remotely to avoid undesirable movements. This procedure was repeated until the specimen completed the maximum deformation of 10 mm. Each deformed body image obtained in the test was named $I_n(x, y)$ with n varying from 1 to 10 (n = 1.10), generating a package of 11 images for each repetition of the experimental test.

Then, the procedure for image processing was initiated to obtain the deformation field of the specimen through the Laser Triangulation method, by applying ImageJ and Excel software. The procedure started based on the image of the reference plane ($I_0(x, y)$) and consisted of: 1 – delimitating the region of the disk where the laser was projected; 2 – Converting the RGB image to grayscale (8-bits); 3 – Gaussian type image filtering; 4 – obtaining the total deformation captured by the LTT in pixel units. This initial procedure generated a routine, obtained by the ImageJ software itself, which was applied to the images referring to the deformed body. Then, ImageJ software exported the reading data to "XLS" files to be worked on in Excel program.

The Excel software was responsible for converting the objects topography data from pixel unit to scalar unit (mm). Conversion was obtained through the ratio between the point where the deformation was imposed (δ_{LTT}) and where its respective luminous intensity occurred (pixel). This relationship is unique for each deformation imposed and is able to be applied on all points of light intensity along the disc. Subsequently, a deformation curve graphic was generated by Excel software and its respective equation was determined.

A correction had to be done on interference related to displacement metallic support (δ_{SM}). This correction index was obtained by the comparator clock, through Equation 01 and resulted in final disk displacement (Δ_{LTT}).

$$\Delta_{LTT} = \delta_{LTT} - \delta_{SM} \, [mm] \tag{1}$$

To analyze the reliability of the data obtained by LTT, the results were compared with two techniques, one of a theoretical nature (Computational Simulation) and the other of a practical nature (Electrical Sensors).

A computational simulation, based on the Finite Element Method (FEM), was carried out to determine the theoretical mechanical behavior expected for the test carried out in the laboratory. In this step, a virtual modelling was generated on Abaqus software, which adopted material properties of specimen and simulated the same condition of real experimental tests (Figure 2). This technique generated theoretical curve deformation, as well as its respective equation. These data were compared with curve deformation and equation curve obtained by LTT to analyze its practical reliability results. Also, FEM determined the possibility of plastic deformation for each deformation imposed.

Figure 2 - Virtual experimental test generated on Abaqus software
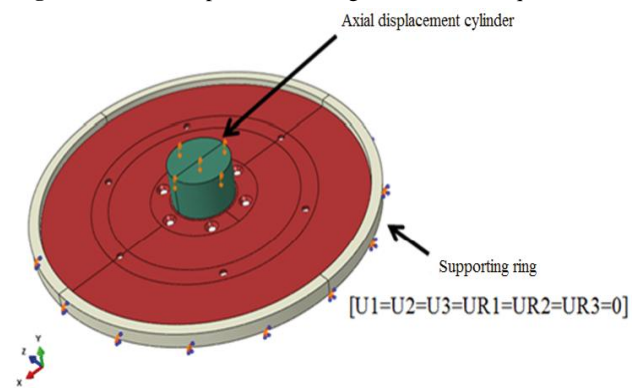
Source: prepared by author (2023)

LTT results of maximum deformation were compared with data obtained by electrical sensors. These practical data were obtained by the load cell transducers of the Universal Testing Machine. As for the LTT, the disc deformation also needed to undergo a data correction due to the deformation of the metallic support. In this case, the disk deformation (Δ_{SE}) was calculated through the difference between the displacement of the load cell captured by the electrical sensor (δ_{SE}) and the displacement of the metallic support (δ_{SM}), through Equation (2).

$$\Delta_{SE} = \delta_{SE} - \delta_{SM} \left[mm \right] \tag{2}$$

The relative error between the deformation data obtained by the LTT and the sensor was determined as a parameter base to analyze the accuracy of the analyzed technique (Equation 3). In this case, the data were punctual and based on the displacement of the load cell.

$$Error_{(\%)} = \frac{\left| \Delta_{SE} - \Delta_{LTT} \right|}{\Delta_{SE}} \times 100 \left[\% \right] \tag{3}$$

RESULTS AND DISCUSSION

Computer Simulation

Firstly, this article shows computer simulation to obtain expected theoretical results of deformation, as well as to determine that loading imposed on the physical specimen would not promote plastic deformation. Figure 3 shows the results of the computer simulation for the deformation field for applied deformation of 10 mm. Figure 4 shows the result of a plastic strain analysis obtained by computer simulation based on the joint strain analysis obtained by Von Mises stresses (PEEQ). The plastic deformation simulation was based on the maximum deformation of 10 mm as the analysis parameter.

Laser Triangulation Technique (LTT)

Figure 5 shows the results of the disk topography for the displacements of 2, 4, 6, 8, and 10 mm, respectively, obtained by image processing using the ImageJ software. For a better understanding and qualitative comparison of the results, the non-deformed disc profile (0.0 mm) was plotted together with the deformed disc profile.

Figure 6 shows the data on the deformation curves of the disc along its entire diameter and length with the trend line plotted for three imposed deformation indices, with a low strain index (3.0 mm), a medium strain index (6.0 mm), and one high strain index (10.0 mm), in addition to the curve of the non-deformed body. Table 1 shows the equations of the deformation curve of the disk, obtained by LTT and by computer simulation.

Figure 7 shows the comparison between strain curves obtained by LTT and computer simulation for

Figure 3 - Deformation field obtained by computer simulation results for 10 mm
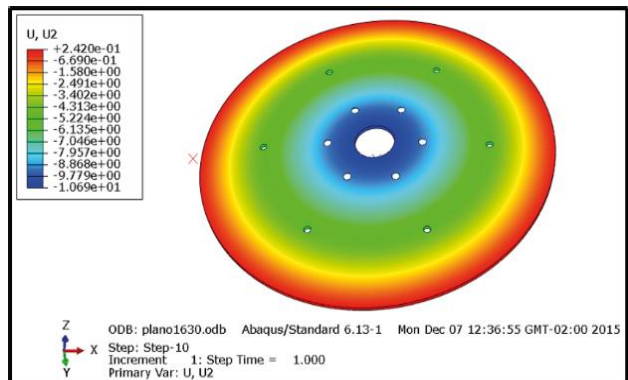
Source: prepared by author (2023)

Figure 4 - Plastic deformation analysis obtained by computer simulation using Von Mises Stresses for 10 mm of deformation
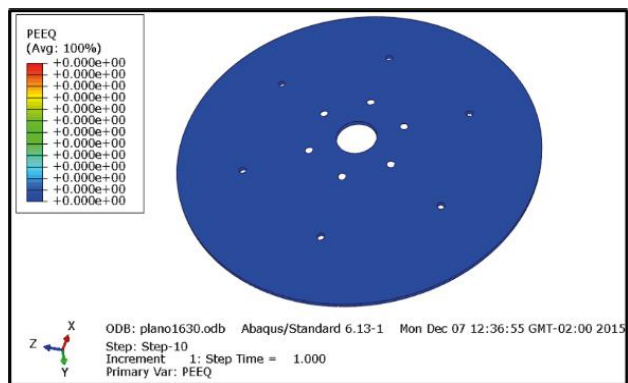
Source: prepared by author (2023)

Figure 5 - Comparison between the non-deformed and deformed laser line profile for the axial displacement for: a) 2 mm; b) 4 mm; c) 6 mm; d) 8 mm; e) 10 mm

Source: prepared by author (2023)

all imposed strain indices. Figure 8 compares the disc deformation curves for three imposed deformation indices, a low strain index (3.0 mm), a medium strain index (6.0 mm) and a high strain index (10.0 mm), besides the curve of the nondeformed body.
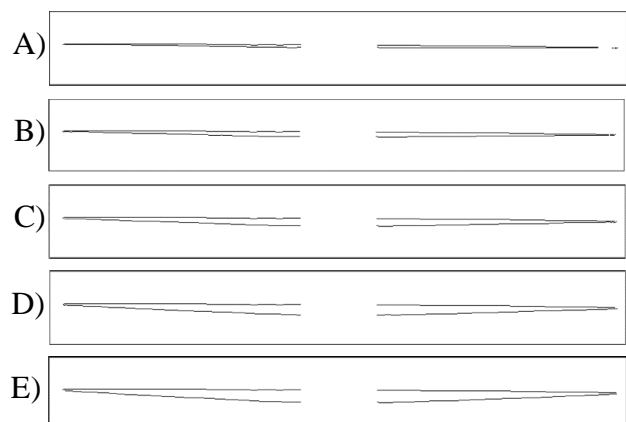
The punctual results in some locations on the horizontal axis of the disk (L.D.) were also compared to the theoretical (Computer Simulation) and experimental (LTT) results, as well as the difference in reading ($|\Delta|$). Table 2 shows this quantitative reading analysis between the analyzed techniques for low strain index (3.0 mm), medium strain index (6.0 mm), and high strain index (10.0 mm).

**Figure 6** - Trend line plotted for the Deformation Curve obtained by LTT
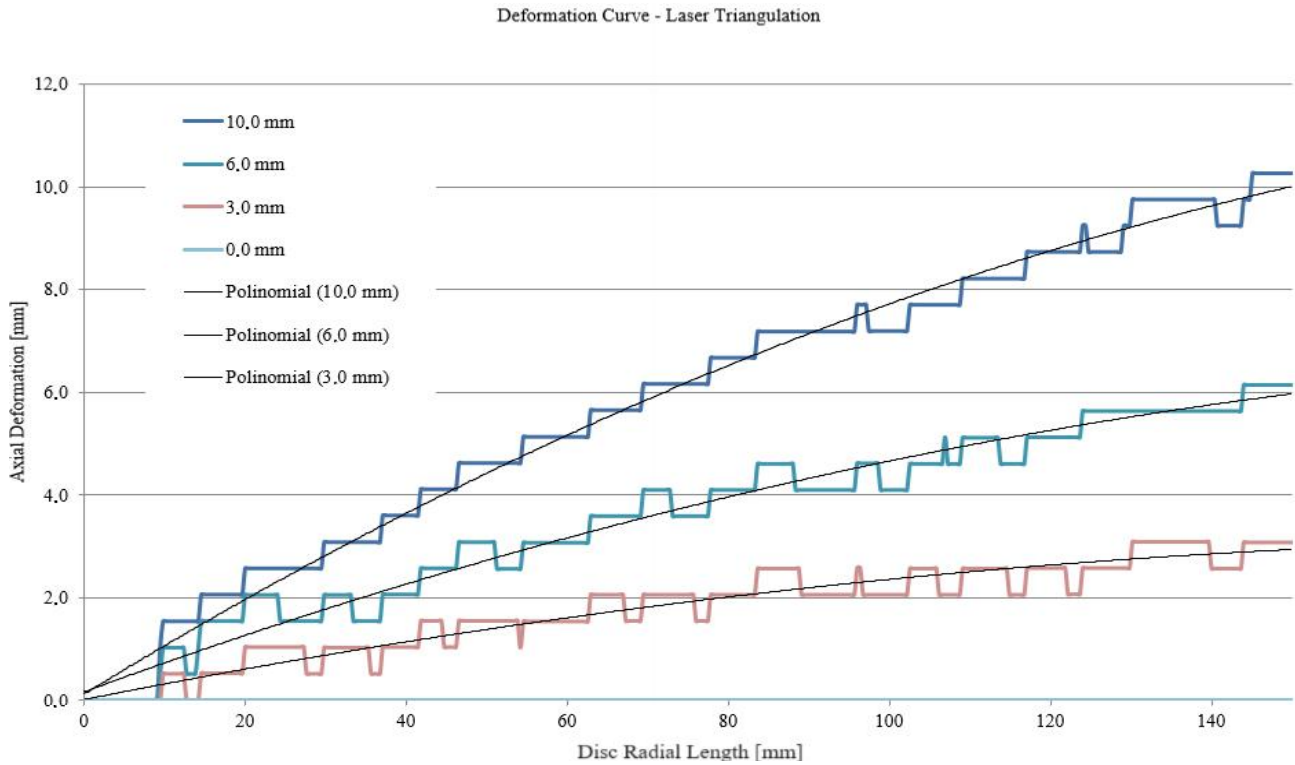
Source: prepared by author (2023)

Table 1 – Deformation curve obtained by LTT and by Computer Simulation

| Deform. Index [mm]	LTT		Computer Simulation	
	Deformation Curve Function ($y = ax^2 + bx + c$)	R^2	Deformation Curve Function ($y = ax^2 + bx + c$)	R^2
1.00	$-0.00004x^2 + 0.0119x + 0.0121$	0.616	$-0.00003x^2 + 0.0107x - 0.0019$	0.99
2.00	$-0.00004x^2 + 0.0187x + 0.0056$	0.863	$-0.00005x^2 + 0.0203x - 0.0031$	1.00
3.00	$-0.00008x^2 + 0.0312x + 0.0195$	0.926	$-0.0001x^2 + 0.038x - 0.0004$	1.00
4.00	$-0.0001x^2 + 0.0407x + 0.0434$	0.955	$-0.0001x^2 + 0.0482x - 0.005$	1.00
5.00	$-0.0001x^2 + 0.0522x + 0.0269$	0.975	$-0.0002x^2 + 0.062x - 0.0022$	1.00
6.00	$-0.0001x^2 + 0.0574x + 0.0173$	0.969	$-0.0002x^2 + 0.0721x - 0.0009$	1.00
7.00	$-0.0002x^2 + 0.0685x + 0.0521$	0.981	$-0.0003x^2 + 0.0845x - 0.003$	1.00
8.00	$-0.0002x^2 + 0.0817x + 0.0974$	0.987	$-0.0003x^2 + 0.0952x + 0.0023$	1.00
9.00	$-0.0002x^2 + 0.0848x + 0.0478$	0.987	$-0.0002x^2 + 0.0881x - 0.0059$	1.00
10.00	$-0.0002x^2 + 0.0960x + 0.0994$	0.989	$-0.0004x^2 + 0.1309x - 0.0015$	1.00

Source: prepared by author (2022)

Figure 7 - Flat disk deformation curve obtained by: a) LTT; b) Computer Simulation
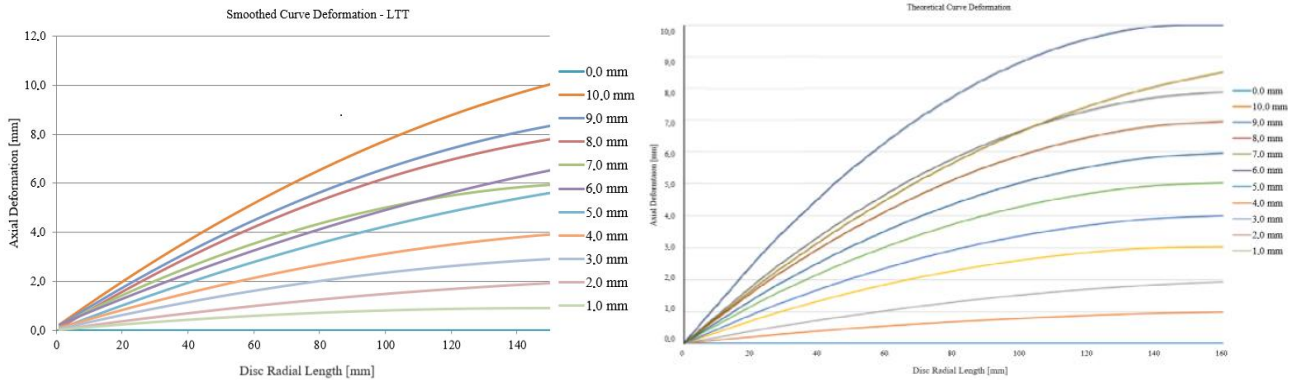
Source: prepared by author (2022)

Figure 8 - Comparative curve deformation obtained by computer simulation and laser triangulation technique
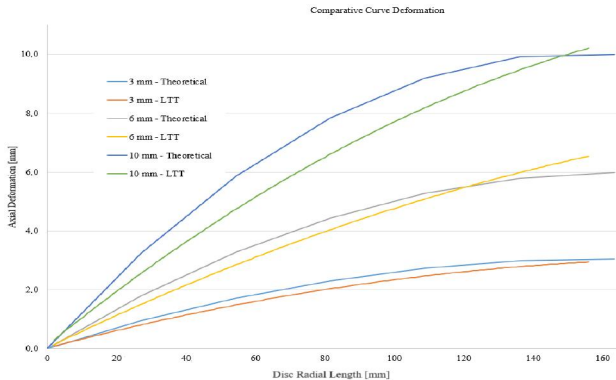
Source: prepared by author (2022)

Electrical Extensometry

Table 3 shows the deformation data obtained by optical and mechanical tests (electrical sensors). In addition, we present data on disc deformation for the mechanical and optical testing, as well as the relative error between the deformation data obtained by LTT and the real data.

By analyzing the deformation behavior of the disc (Figure 3), one should expect non-linearity from the deformation behavior of the body, because the color variation along the disc does not have bands of the same length. The deformations on the edge of the disc under the metallic disc are expected to present lower deformation indices and the higher deformation indices are expected to be concentrated near the center of the disc. Computer simulation illustrated on Figure 4 showed that a deformation up to 10 mm would not be enough to

cause plastic deformations, indicating that the specimen obeys Hooke's law. Then, it is possible to affirm that the curve equations for the practical LTT tests obtained in experimental tests can serve as a basis for determining the deformation field of the disc.

Analyzing the results of the optical test, in Figure 5, the LTT qualitatively showed that metallic disc deformation was in common agreement with expected theoretical results, with a low deformation index on the outer edge of the disc and higher deformation indices in the central part, where the load cell is applied. It is also noted that the outer edge of the disc showed a slight and increasing displacement as the deformation applied to the specimen was enlarged. The deformation curve presented in Figure 6 shows that the data obtained by LTT had a sawn shape. This was due to noise occurring during the image capturing and processing. These noises are smoothed by plotting the curve's trend line and with precision data evaluated by its squared error (R^2). Comparing the curve functions obtained between the LTT and the computer simulation, it is noted that the factors were very close with small variations in the indices (a, b and c) with values that are not very distorting, that is, the equations are very close to each other, producing very little distortions between theoretical and practical results. The R^2 of the computer simulation was around 100%, and the disk did not have any plastic deformation developed, as illustrated in Figure 7; therefore, it can be said that the curve equation faithfully portrays the formulated theoretical deformation equation by the strength of materials.

The R^2 for LTT was low for small strains but got higher as strain increased, reaching close to 100%. This improvement in data accuracy is due to the fact that the

greater the deformation imposed on the specimen, the greater the clarity in the image subtraction process and, consequently, the lower the noise interference in the image capturing process. This allows us to say that, for LTT, larger deformations can imply greater data accuracy. With the proximity between the equations the LTT results suggest a good degree of precision and reliability.

Table 2 - Modular difference (Δ) in reading between theoretical results obtained by computer simulation (CS) and by the laser triangulation technique (LTT) for imposed deformations (δ) of low, (3.0 mm), medium (6.0 mm) and high strain index (10.0 mm)

L.D.	δ = 3.0 mm			δ = 6.0 mm			δ = 10.0 mm		
	C.S.	LTT	$|\Delta|$	C.S.	LTT	$|\Delta|$	C.S.	LTT	$|\Delta|$
10	0.3696	0.3235	0.0461	0.7001	0.5813	0.1188	1.2675	1.0394	0.2281
20	0.7196	0.6115	0.1081	1.3611	1.1253	0.2358	2.4565	1.9394	0.5171
30	1.0496	0.8835	0.1661	1.9821	1.6493	0.3328	3.5655	2.7994	0.7661
40	1.3596	1.1395	0.2201	2.5631	2.1533	0.4098	4.5945	3.6194	0.9751
50	1.6496	1.3795	0.2701	3.1041	2.6373	0.4668	5.5435	4.3994	1.1441
60	1.9196	1.6035	0.3161	3.6051	3.1013	0.5038	6.4125	5.1394	1.2731
70	2.1696	1.8115	0.3581	4.0661	3.5453	0.5208	7.2015	5.8394	1.3621
80	2.3996	2.0035	0.3961	4.4871	3.9693	0.5178	7.9105	6.4994	1.4111
90	2.6096	2.1795	0.4301	4.8681	4.3733	0.4948	8.5395	7.1194	1.4201
100	2.7996	2.3395	0.4601	5.2091	4.7573	0.4518	9.0885	7.6994	1.3891
110	2.9696	2.4835	0.4861	5.5101	5.1213	0.3888	9.5575	8.2394	1.3181
120	3.1196	2.6115	0.5081	5.7711	5.4653	0.3058	9.9465	8.7394	1.2071
130	3.2496	2.7235	0.5261	5.9921	5.7893	0.2028	10.2555	9.1994	1.0561
140	3.3596	2.8195	0.5401	6.1731	6.0933	0.0798	10.4845	9.6194	0.8651
150	3.4496	2.8995	0.5501	6.3141	6.3773	0.0632	10.6335	9.9994	0.6341

Source: prepared by author (2022)

Table 3 - Relative error of deformation between electronic sensor and LTT

Digital Dial Gauge	Mechanical Testing (Sensors)		Laser Triangulation Technique (LTT)		Relative Error [%]
δSM [mm]	δSE. [mm]	ΔSE [mm]	δLTT [mm]	ΔLTT [mm]	
0.00	0.00	0.00	0.00	0.00	0.00
0.00	1.00	1.00	1.02	1.02	2.00
0.01	2.00	1.99	2.05	2.04	2.51
0.01	3.00	2.99	3.07	3.06	2.34
0.02	4.00	3.98	4.11	4.09	2.76
0.05	5.00	4.95	5.13	5.08	2.62
0.07	6.00	5.93	6.16	6.09	2.69
0.10	7.00	6.90	7.17	7.07	2.46
0.13	8.00	7.87	8.21	8.08	2.67
0.18	9.00	8.82	9.23	9.05	2.60
0.23	10.00	9.77	10.25	10.02	2.56

Source: prepared by uthor (2022). δ_{SM} - Deformation of the metallic support; δ_{SE} - Total disk displacement; Δ_{SE} - Disc deformation; δ_{LTT} - Total disk displacement obtained by LTT; Δ_{LTT} - Disc deformation obtained by LTT

By analyzing Figure 7, we noted that the deformation curve for the LTT, obtained through the curve equation, showed a behavior similar to the theoretical curve, mainly for the lower deformation indices, but they clashed as the imposed deformation was expanded, as can be seen in Figure 8. We also noted that, for both curves, there was a moment when the deformation curves intersect (6.0 – 7.0 mm: experimental / 8.0 – 9.0 mm: theoretical) and points close to the radial length of the disc (110.0 mm), thus maintaining a similarity between the practical and theoretical results. Hence the fact that the curves crossed would not be an abnormality of the experimental curve.

The quantitative difference in reading between techniques, shown in Table 2, indicates a maximum value of 1.42 mm for high strain index (10.0 mm). This difference can be explained by the fact that, in practice, the body is not integral in its material constitution, that is, there are internal flaws, and, with a high rate of imposed deformation, distortions have increased. On average, these differences were much smaller than 1.0 mm, which shows a high degree of approximation between the theoretical and the practical data. In general, even if there was a difference between the curve equations, which is reflected by deformation data, such a disparity would already be expected, as in computer simulations there is no possibility of embedding the particularities an object may have, such as internal flaws, irregularity in the format, among others.

The displacement field can be represented by approximate functions and the principle of minimum potential energy is used, the unknowns are identified as the nodal displacement, and the analysis method is referred to as displacement model or stiffness model (SMITH NETO, 2005). Therefore, the curve equations for each model can predict the approximation between disk deformation data. Silva, Gazzola and Dal Fabbro (2013) carried out experimental tests and compared them with theoretical results for single and double crimped beams, respectively, and they found out that the theoretical curves are approximations of the real deformation behavior that a body may suffer, and they pointed to mismatches between theoretical and practical data in their deformation curves.

The data in Table 3 indicate that the relative error was at least 2%, however, it did not exceed 3% for the other readings. It is also noted that from the displacement data of the dial indicator that, as the applied load increased, the deformation of the metallic support affected the displacement of the disk, as shown in Figure 4. Therefore, the LTT showed sensitivity by presenting the need of the displacement of the specimen and capture the complete set displacement. By analyzing the relative error data presented, it is also noted there was no pattern of growth of the relative error in relation to the deformation rate of the body, showing that the source of the error between the real data and the theoretical data used is in the image capture stage, which generates certain noise, as well as its processing, in which the crossing of images can generate certain image disturbances and, consequently, disturb their results. However, even with this difference, which was already expected, and, based on the ISO 15530 standard, which determines that the profilometry of a body obtained by measurements should not exceed 5% of the real value of the object (SILVA; GAZZOLA; DAL FABBRO, 2012), it still generates reliable and accurate data. For Kesner *et al.* (2021), the divergence between practical and theoretical results was close to 20%, which he considered acceptable. The accuracy data for this article were close to those obtained by Shen *et al.* (2013).

Due to the fact that the data obtained with the experimental technique was so close to the theoretical result that considers the material to be perfect in material and superficial terms, it can be noted that the technique is highly accurate. Its advantage is that the material particularities can be built into the results, and design problems can be predicted, resulting in safer products, as well as in the development of more optimized parts.

CONCLUSIONS

1. Based on what was presented above, it is concluded that the reliability of the Laser Triangulation Technique (LTT) to determine the deformation of a specimen proved to be satisfactory. Such statement can be made based on the following observations: similar strain curve behavior between practical and theoretical results; unpredictable inversion behavior between the deformation curves (6.0 – 7.0 mm) for the practical result was also recurrent in the theoretical results (8.0 – 9.0 mm) and at points close to the radial length of the disc (110.0 mm); factors a, b and c of the strain curve equation had similar values; the points of greatest difference between theoretical and practical readings were highest in the middle region of the disc and the smallest in the extreme regions of the body; the possibility of obtaining the deformation curve by analyzing the material quality of the body, such as anisotropies, internal flaws, among other particularities that a computer simulation does not allow it to be easily embedded;

2. Therefore, one must pay attention to the fact that the analysis of the efforts that a body undergoes and—according to its complexity—when combined with theoretical analysis and experimental techniques, can provide information of great importance for the development of optimized and safer parts and machines, mainly to farm machineries. It is recommended that, for the use of the experimental technique, low strain indices should be used.

REFERENCES

CARDOSO, K. C.; GAZZOLA, J.; DAL FABBRO, I. M. Application of moiré technique on strain analysis in farm machinery elements. **Revista Ciência Agronômica**, v. 45, p. 479-487, 2014.

DONG, Z. *et al*. Measurement of free-form curved surfaces using laser triangulation. **Sensors**, v. 18, p. 3527, 2018.

GÜRSOY, S.; CHEN, Y.; LI, B. Measurement and modelling of soil displacement from sweeps with different cutting widths. **Biosystem Engineering**, v. 161, p. 1-13, 2017.

HUAN, H. *et al*. Mechanical strength evaluation of elastic materials by multiphysical nondestructive methods: a review. **Applied Science**, v. 10, p. 1588, 2020.

KESNER, A. *et al*. Stress distribution on a soil tillage machine frame segment with a chisel shank simulated using discrete element and finite element methods and validate by experiment. **Biosystem Engineering**, v. 209, p. 125-138, 2021.

KIENLE, P. *et al*. Increasing the sensitivity of laser triangulation systems using structured optical surfaces. **Proceedings of SPIE**, 2020. DOI:10.1117/12.2566094.

MAZZETI, V. *et al*. Application of a moiré technique in the stress distribution mapping of circular rotors. **Revista Ciência e Tecnologia**, v. 1, n. 10, p. 31-34, 2004.

MORENO-OLIVA, V. I. *et al*. Measurement of quality test of aerodynamic profiles in wind turbine blades using laser triangulation technique. **Energy Science & Engineering**, v. 7, n. 5, 2019.

MORENO-OLIVA, V. I. *et al*. Vibration measurement using laser triangulation for applications in wind turbine blades. **Simmetry**, v. 13, n. 6, 2021.

NATRAYAN, L. *et al*. Analysis and optimization of connecting tie rod assembly in agricultural application. **Acta Mechanica**, v. 3, n. 1, p. 6-10, 2019.

NIEMCZEWSKI, B. K. *et al*. Validação de um modelo de cálculo por elementos finitos do chassi de uma semeadora de quatro linhas. **Engenharia Agrícola**, v. 34, n. 1, p. 161-170, 2014.

PAN, B. Digital mage correlation for surface deformation measurement: historial developments, recent advances and future goals. **Measurement Science and Technology**, v. 29, n. 8, 2018.

SHEN, L.; LI, D.; LUO, F. Study on laser speckle correlation method applied in triangulation displacement measurement. **Journal of Optical Technology**, v. 80, n. 10, p. 604-610, 2013.

SIEKANSKI, P. *et al*. On-line laser triangulation scanner for wood logs surface geometry measurement. **Sensors**, v. 19, n. 5, 2019.

SILVA, M. V. G.; GAZZOLA, J.; DAL FABBRO, I. M. Uso de técnicas ópticas de moiré para determinação prática do comportamento de vigas estruturais. **Revista Funec Científica: Multidisciplinar**, v, 2, n. 3, p. 1-16, 2012.

SMITH NETO, P. **Fundamentos para o Projeto de Componentes de Máquinas**. San Francisco: Ed. Creative Commons, 2005. 464 p.

XIANG, S. *et al*. Melt level measurement for the CZ crystal growth using an improved laser triangulation system. **Measurements**, v. 103, p. 27-35, 2017.

XIE, L. *et al*. Optimisation and finite element simulation of the chopping process for chopper sugarcane harvesting. **Byosistem Engineering**, v. 175, p. 16-26, 2018.

ZULKIFLI, N. *et al*. Finite element for fruit stress analysis: a review. **Trends in Food Science & Technology**, v. 97, p. 29-37, 2020.